AWARD NUMBER: W81XWH-16-1-0397

TITLE: Large Oncosomes: A Novel Liquid Biopsy for Genetic Profiling in Patients with Castration Resistant Prostate Cancer

PRINCIPAL INVESTIGATOR: Dolores Di Vizio, MD, PhD

CONTRACTING ORGANIZATION: Cedars-Sinai Medical Center, Los Angeles, CA

REPORT DATE: December 2019

TYPE OF REPORT: Final

PREPARED FOR: U.S. Army Medical Research and Materiel Command
Fort Detrick, Maryland 21702-5012

REPORT DOCUMENTATION PAGE

Form Approved
OMB No. 0704-0188

1. REPORT DATE *(DD-MM-YYYY)*	2. REPORT TYPE	3. DATES COVERED *(From - To)*
December 2019	Final	01Sep2016-31Aug2019

4. TITLE AND SUBTITLE
Large Oncosomes: A Novel Liquid Biopsy for Genetic Profiling in Patients with Castration Resistant Prostate Cancer

5a. CONTRACT NUMBER
W81XWH-16-1-0397

5b. GRANT NUMBER

5c. PROGRAM ELEMENT NUMBER

6. AUTHOR(S)
Dolores Di Vizio, MD, PhD

email - Dolores.DiVizio@cshs.org

5d. PROJECT NUMBER

5e. TASK NUMBER

5f. WORK UNIT NUMBER

7. PERFORMING ORGANIZATION NAME(S) AND ADDRESS(ES)
Cedars-Sinai Medical Center
8700 Beverly Blvd
Los Angeles, CA 90048-1804

8. PERFORMING ORGANIZATION REPORT NUMBER

9. SPONSORING/MONITORING AGENCY NAME(S) AND ADDRESS(ES)
US Army Medical Research and Material Command
Fort Detrick, Maryland 21702-5012

10. SPONSOR/MONITOR'S ACRONYM(S)

11. SPONSOR/MONITOR'S REPORT NUMBER(S)

12. DISTRIBUTION/AVAILABILITY STATEMENT
Approved for Public Release; Distribution Unlimited

13. SUPPLEMENTARY NOTES

14. ABSTRACT
The overarching goal of my laboratory is to investigate whether circulating LO, a novel class of atypically large (1-10μm diameter), bioactive extracellular vesicles (EVs), which are released by highly invasive and metastatic amoeboid tumor cells in the plasma, and contain abundant RNA, miRNA, DNA, and protein cargo, report clinically relevant information and tumor-specific genomic alterations, thus representing a valuable alternative and/or complement to other technologies proposed as a means of liquid biopsy. Collectively our findings indicate that DNA analyses of LO in blood (plasma) may provide a faithful representation of the genome of the tumor cells of origin Because we have performed also

15. SUBJECT TERMS
Metastatic Castration Resistant Prostate Cancer, Extracellular Vesicles, Extracellular DNA, Large Oncosomes, Next Generation Sequencing, Liquid Biopsy, digital droplet PCR

16. SECURITY CLASSIFICATION OF:			17. LIMITATION OF ABSTRACT	18. NUMBER OF PAGES	19a. NAME OF RESPONSIBLE PERSON
a. REPORT	b. ABSTRACT	c. THIS PAGE			USAMRMC
unclassifed	unclassifed	unclassifed	unclassifed	10	19b. TELEPHONE NUMBER *(Include area code)*

TABLE OF CONTENTS

Accomplishments

During the first year of the DoD funding, we identified molecules whose alterations are responsible for nuclear membrane instability and provided evidence that this results in the shedding of EVs that contain nuclear material. During the second year of the DoD funding, these results were published [1]. During the second year of funding, we determined the size of the intact vesicular DNA, which supports our hypothesis that EVs can contain nuclear material. To accomplish this, we lysed EVs directly in agarose plugs and resolved EV DNA by pulse-field gel electrophoresis (PFGE). Resolution of high molecular weight DNA, which was possible with this method, revealed that L-EVs contain DNA fragments up to 2 Mbp (**Figure 1A**). In addition, DNA fragments in the size range of 100 Kbp–2 Mbp were enriched in L-EVs compared to whole cells and were undetectable in S-EVs (**Figure 1A**). This is in agreement with our previous results suggesting a distinct process of DNA packaging in L-EVs. We have also analysed the high molecular weight DNA contained in plasma-derived EVs. Even though the amount of EV DNA obtained from 1 ml of plasma was significantly lower than the amount of DNA in our *in vitro* system, the size of the intact DNA in plasma-derived L-EVs was in the size range of 100 kbp–2 Mbp (**Figure 6B**), replicating our *in vitro* findings. The amount of DN A in S-EVs was, again, undetectable.

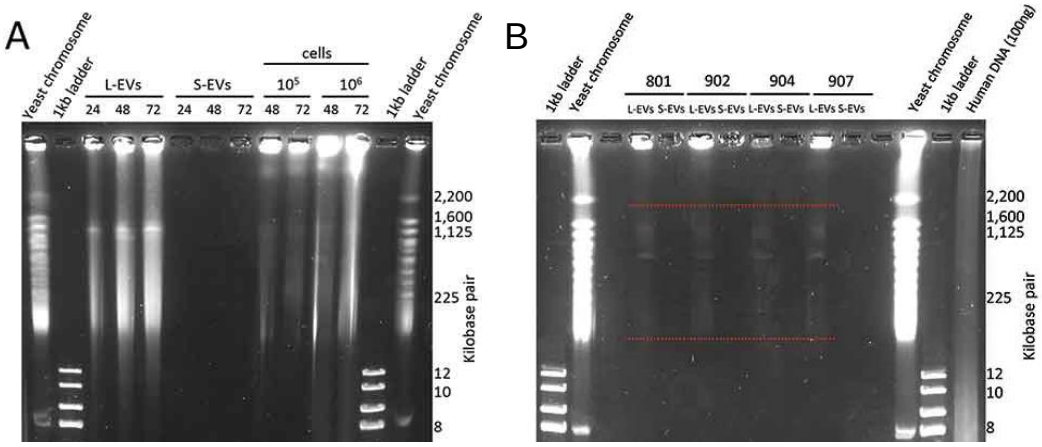

Figure 1. EVs contain high molecular weight DNA. A. PC3 L-EV and S-EV DNA was extracted in agarose plugs by incubation in lysis buffer for 24, 48 or 72 h, and high molecular weight DNA was resolved by PFGE, which revealed that L-EVs contain large DNA fragments (100 kbp–2 Mbp). **B**. EVs were isolated from 1 ml of plasma obtained from mCRPC patients, EV DNA was extracted in agarose plugs by incubation in lysis buffer for 48 h, and high molecular weight DNA was resolved by PFGE. Similar to L-EVs *in vitro*, patient plasma-derived L-EVs contain high molecular weight DNA (100 kbp–2 Mbp) (indicated by red dashed lines).

In the third year of the DoD-funded project, we performed the very first large-scale DNA analysis of two distinct extracellular vesicle (EV) populations, large (L-) and small (S-)EVs, isolated from 2ml plasma specimens obtained from two patients with metastatic castration resistant prostate cancer (mCRPC). For each patient, sequencing data/genetic profile of matching metastatic tissue biopsy was available to us through Dr. Edwin Posadas at Cedars-Sinai Medical Center. L- and S-EVs were isolated by differential centrifugation. Total amount of dsDNA in the L-EV fractions was 7.32 ng and 228.3 ng, in the S-EV fractions the amount of dsDNA was 9.33 ng and 3.45 ng, respectively. After standard quality control of the EV

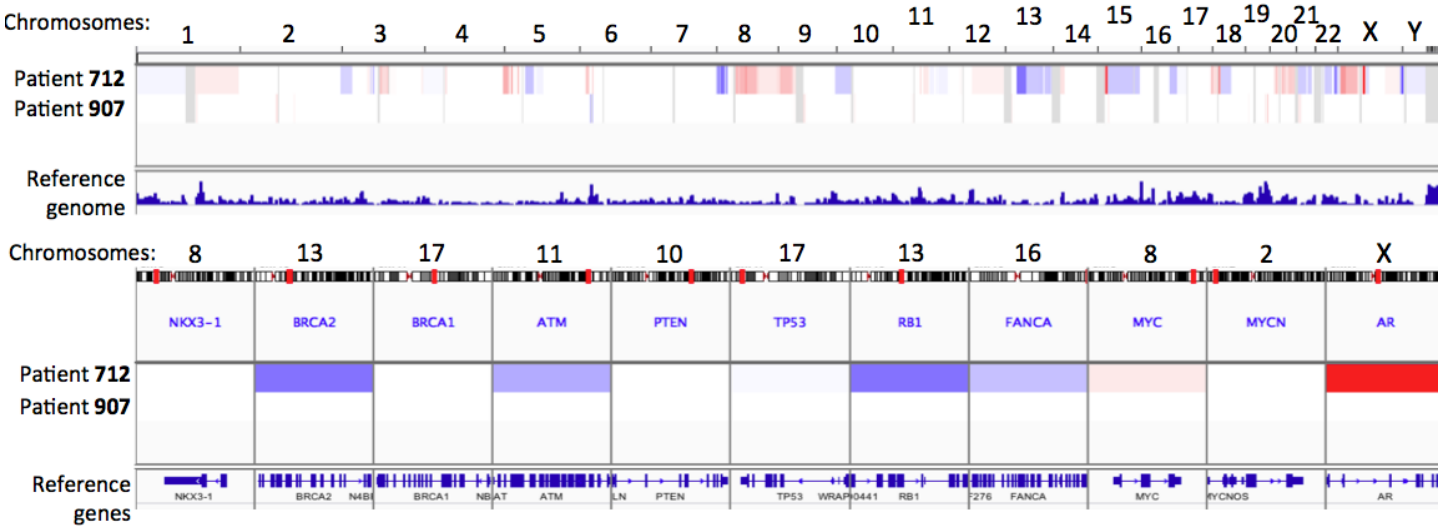

Figure 2. EV-associated DNA reflects typical for mCRPC genomic alterations. Upper panel shows genetic landscape across all chromosomes; amplifications are marked in red, deletions are marked in blue. Lower panel shows genomic aberrations in individual genes commonly altered in mCRPC.

DNA samples, whole exome sequencing at 1500-2000x was performed at the Genomics Resources Core Facility at Weill Cornell Medical College, New York, USA. Germline DNA (buffy coat) from each patient was used as control. For data analysis of this highly reach sequencing, we established a collaboration with Dr. Francesca Demichelis, University of Trento, Italy. Dr. Demichelis has established a pipeline for analysis of sequencing data on cell free (cf)DNA [2,3]. Somatic copy number aberrations and mutations specific for mCRPC were identified.

In the L-EV DNA from one of the two patients, a tissue-quality tumor signal showing 65% tumor purity and 2.86 ploidy was detected. Moreover, this tumor signal was represented by typical mCRPC genomic alterations, such as amplifications of *AR* and *MYC*, and deletions in *BRCA2* and *RB1* (**Figure 2**). When we compared these results with the results of the FoundationOne test, which detects all classes of genomic alterations in more than 300 cancer-related genes, on the matched tumor tissue from this patient, we identified the same alterations (e.g. *AR* amplification, *BRCA2* deletion). Importantly, plasma L-EV DNA reported additional mCRPC-specific genomic aberrations that had not been detected in the tissue biopsy (e.g. *MYC* amplification, *RB1* deletion). This suggests that the DNA associated with circulating L-EVs might be more informative in comparison with the DNA extracted from tissue biopsy, because it contains genetic information from different metastases throughout the body. The S-EV DNA from the same patient exhibited a similar profile (not shown).

We have demonstrated that most of the tumor DNA circulating in prostate cancer patient plasma is associated with L-EVs [4]. However, the tumor signal detected in the L-EV fraction might also arise from the circulating cfDNA, which might co-precipitate with L-EVs or/and be associated with the EV surface. To find out if the tumor signal detected in the L-EV fraction originates from the DNA content of these vesicles (and, thus, may provide different from the circulating cell-free tumor DNA information), we (i) developed a nuclease treatment protocol for EVs, to get rid of extravesicular DNA, and (ii) established a system that allows us to distinguish between the extravesicular DNA and the DNA contained inside the EVs.

(i) First, we treated the samples with nucleases, DNaseI and ExoIII, to quantitatively assess the amount of extravesicular and intravesicular EV-associated DNA. Briefly, EVs from PC3 cell line were spiked into 1 ml of plasma obtained from healthy donors. L- and S-EV fractions were isolated from plasma specimens and DNA was extracted either from EVs directly, without any pre-treatment, or following pre-treatment with nucleases (**Figure 3A**). We observed that the amount of DNA recovered from either L- or S-EV fractions was substantially reduced when EVs had been pre-treated with nucleases (**Figure 3A**). This result suggested that a large portion of EV DNA is extravesicular and accessible to nucleases. We also confirmed the presence of the extravesicular DNA on the surface of EVs, as well as EV integrity following treatment with nucleases, by flow cytometry (**Figure 3B**). Intact EVs, untreated or following nuclease treatment, were immunofluorescently labeled using the antibody that specifically recognized dsDNA and fluorescence was analyzed by flow cytometry. As expected, a population of dsDNA-positive EVs was

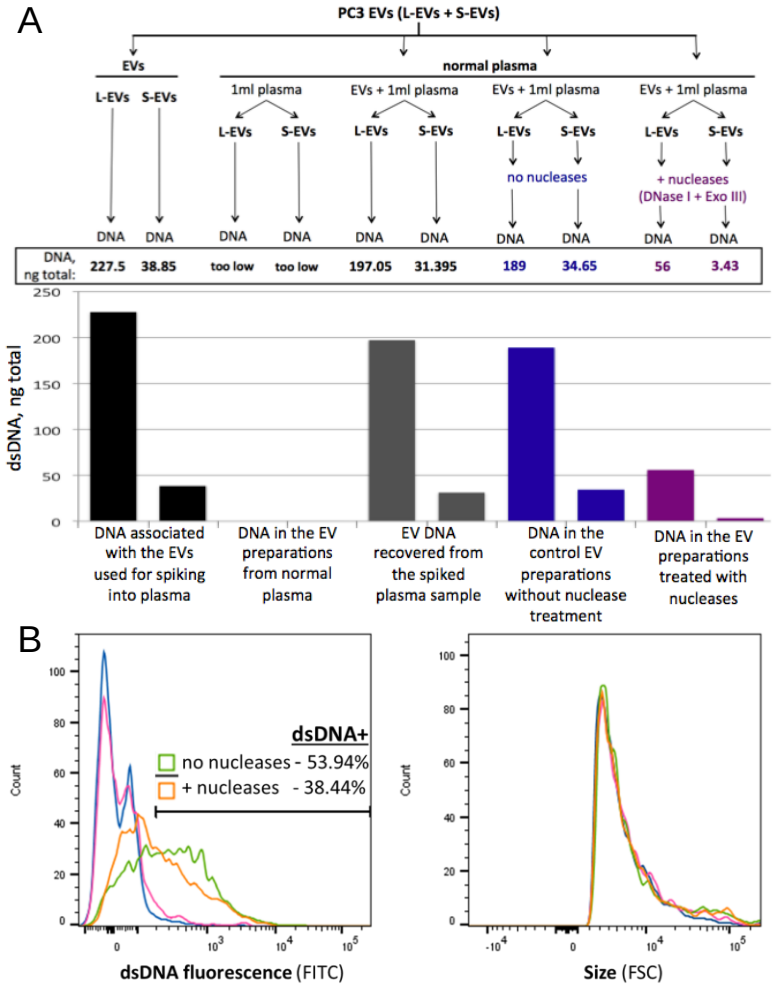

Figure 2. Large portion of EV-associated DNA is extravesicular. **A**. Experimental design and quantification of the results of the spike-in experiment. PC3-derived EVs were spiked into 1 ml of plasma from healthy donors. Following EV isolation by ultracentrifugation, the EV DNA was extracted with or without pre-treatment with nucleases. The DNA yield was quantified by High Sensitivity dsDNA Qubit Assay. **B**. Intact EVs were immunolabeled with anti-dsDNA antibody and the fluorescence intensity as well as size of the EVs were analyzed by flow cytometry. Pink – unlabeled EVs, blue – no primary control EVs, green – untreated EVs labeled with the dsDNA antibody, yellow – EVs treated with nucleases and labeled with the dsDNA antibody.

detected in the untreated sample (**Figure 3B, left, green line**), while there was a clear shift in the fluorescence towards the dsDNA-negative EV population in the EV sample treated with nucleases prior to immunolabeling (**Figure 3B, left, yellow line**), confirming that a portion of EV DNA is extravesicular and accessible to nucleases. Importantly, both untreated and nuclease-treated EV samples exhibited completely overlapping size distribution profiles (**Figure 3B, right**) confirming that nuclease treatment protocol did not affect the integrity of EVs. Taking together, these results led to conclude that a portion of the DNA is enclosed into EVs, and the relative portion of DNA in L-EVs is higher than in S-EVs – possibly due to the fact that the L-EV volume is ~1,000 times larger than the S-EV volume.

(ii) We next sought to confirm that the DNA that resists nuclease treatment (following pre-treatement with nucleases), is indeed intravesicular. In order to do so, PC3-derived EVs were spiked into 1 ml of plasma from healthy donors together with genomic (g)DNA extracted from non-cancerous cells (primary lung fibroblasts IMR90, ATCC® Number: CCL-186™). PC3 cells exhibit a highly aberrant genome and have a homozygous deletion of *PTEN* among other gains and losses that manifest as somatic copy number variations. Therefore, we reasoned that we would be able to distinguish between the intravesicular PC3 DNA and extravesicuar IMR90 DNA based on the detectability of the *PTEN*, which would be undetectable in the intravesicular PC3 DNA but detectable in the extravesicular IMR90 DNA by digital (d)PCR. Thus, the presence of the *PTEN* dPCR product would indicate the presence of extravesicular DNA in the sample, and the absence of the *PTEN* dPCR product would indicate that only intravesicular DNA is present in the sample. We used dPCR with specific *PTEN* primers to test this hypothesis.

After spiking PC3-derived EVs and IMR90 gDNA into plasma, L- and S-EVs were isolated from the plasma specimens, and DNA was extracted from the EVs directly or following nuclease treatment (**Figure 4**) – like in the previous experiment. In agreement with the previous result, there was a substantial decrease in the amount of DNA obtained from the nuclease-treated EVs (**Figures 3** and **4**). To find out the intra- or extravesicular localization of the EV-associated DNA, dPCR was performed on the L-EV DNA samples and *PTEN* CNV per diploid genome was quantified using RNaseP as a reference gene. We found that *PTEN* transcripts were present in the DNA from the untreated L-EVs, which meant that extravesicular gDNA had co-precipitated with the vesicles and was present in the L-EV DNA sample (**Figure 4, green**). However, *PTEN* transcripts were undetectable in the DNA from the nuclease-treated L-EVs, suggesting that the extravesicular gDNA had been digested by nucleases and only intravesicular DNA was present in the sample (**Figure 4, yellow** and **blue**).

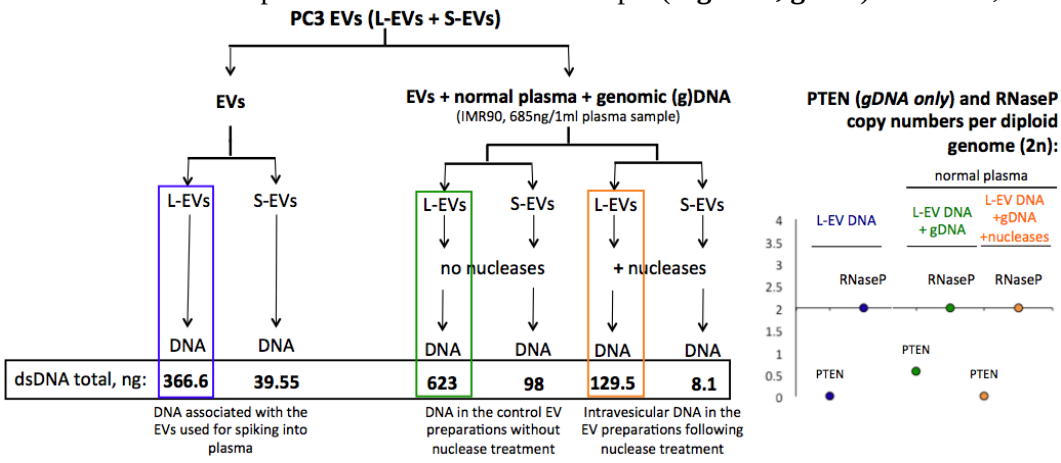

Figure 4. Nuclease treatment digests DNA outside of the EVs leaving the intravesicular DNA intact. The scheme on the left shows experimental design and quantification of the results. PC3-derived EVs and IMR90 gDNA were spiked into 1 ml of plasma from healthy donors. Following EV isolation by ultracentrifugation, the EV DNA was extracted with or without pre-treatment with nucleases. The DNA yield was quantified by High Sensitivity dsDNA Qubit Assay and PTEN copy number per diploid genome was quantified by dPCR (plot on the right).

After we established the nuclease treatment protocol for EVs to get rid of extravesicular DNA and confirmed its efficiency, we next sought to investigate if the DNA inside the L-EVs may provide different tumor-specific genetic information from the circulating cfDNA. In order to address this question, we are compared, side-by-side, the tumor signal in the DNA extracted from (i) plasma (circulating cfDNA), (ii) EVs without nuclease treatment (like in the original experiment), and (iii) EVs treated with nucleases. For this experiment, 6 ml of plasma from three mCRPC patients (provided by our collaborator Dr. Posadas) was split in 3 x 2 ml aliquots. One aliquot was used for the direct extraction of cfDNA (**Figure 5, i**) and the remaining two aliquots were used for EV isolation by differential centrifugation followed by DNA extraction with or without nuclease treatment (**Figure 5,**

ii and iii). The quality control Quality control of the DNA samples was performed using the Agilent 2100 Bioanalyzer High Sensitivity DNA kit (Agilent Technologies) at the Cedars-Sinai's Applied Genomics, Computation and Translational Core and showed the presence of typical nucleosomal DNA fragments in the cfDNA sample (**Figure 5(i)**) which were absent in the EV DNA samples (**Figure 5(ii)** and **(iii)**), confirming better integrity of the EV DNA and suggesting a different underlying biology of these DNA species. Total amount of cfDNA and EV DNA in different fractions is provided in the **Table 1**. The DNA in the S-EV fractions after treatment with nucleases was undetectable, in line with our previous findings that almost all S-EV-associated DNA is extravesicular, and therefore, all S-EV samples were excluded from further analysis. After quality control, DNA libraries were constructed and WES at 1500-2000x was performed at the Genomics Resources Core Facility at Weill Cornell Medical College, New York, USA. Germline DNA (buffy coat) from each patient was used as control. For data analysis, we used our previously established collaboration with Dr. Francesca Demichelis at the University of Trento, Italy,. Somatic copy number alterations (SCNAs) specific for mCRPC were identified in one patient out of three. It was the same patient, 712, in which we identified a high-quality tumor signal in our original WES experiment.

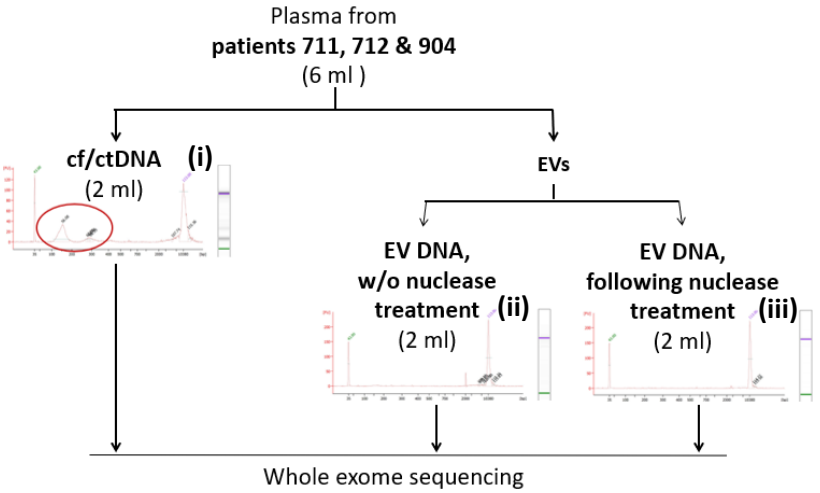

Figure 5. Scheme of the experiment comparing side-by-side tumor-specific genetic information carried by cfDNA versus EV DNA. The integrity of EV DNA is better preserved compared to cfDNA. Nucleosomal DNA fragments typical of cfDNA are indicated by the red circle.

Table 1. Total DNA yield (ng) from different plasma fractions

	cfDNA	EVs, no treatment		EVs treated with nucleases	
		L-EV DNA	S-EV DNA	L-EV DNA + nucl.	S-EV DNA + nucl.
Patient 711	25.1	12.1	3.6	7.65	nd
Patient 712	12.3	8.5	3.2	2.3	nd
Patient 904	40.5	39	5.6	32.1	nd

nd = not detected

The WES demonstrated that mCRPC-specific SCNAs could be detected in both cfDNA and L-EV DNA obtained from 2 ml of patient plasma, but the tumor signal in cfDNA appeared to be more pronounced than in L-EV DNA (**Figure 6**). Similar

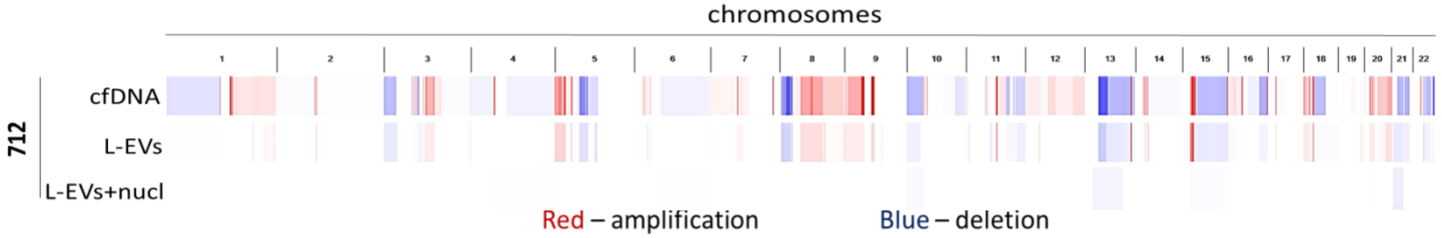

Figure 6. Comparative analysis of the tumor signal in cfDNA vs L-EV DNA in mCRPC patient plasma.

to the original WES experiment, a number of genomic alterations, such as AR, ARFRP1, AURKA, GNAS, and ZNF217 amplifications, were detected both in the circulation by our analysis and in the matched tumor tissue by the FoundationOne test (which detects all classes of genomic alterations in more than 300 cancer-related genes) from this patient. Moreover, the same genomic alterations: AR and MYC amplifications, and RB1, BRCA2, ATM, and FANCA deletions, were detected both in the L-EV DNA in the original experiment and in cfDNA and L-EV DNA in the follow-up experiment confirming the reliability of our findings. Additionally, NKX3-1 deletion was detected in both cfDNA and L-EV DNA in the follow-up but not in the original WES experiment. Finally, in the follow-up WES experiment, PTEN, TP53, and MYCN deletions were found in cfDNA for the first time – none of these alterations were detected in L-EV DNA in both experiments. Unfortunately, due to the very low DNA yield in the L-EVs that had been treated with nucleases (2.3 ng), we couldn't detect a reliable tumor signal in that sample.

In parallel experiments, we sought to establish if L-EVs could also report cancer-specific mutations in another type of cancer – non-small cell lung cancer (NSCLC). Using Tunable Resistive Pulse Sensing technology (qNano Gold, Izon, New

Zealand), we demonstrated that L-EVs are present exclusively in plasma from NSCLC patients and absent in plasma from healthy donors (**Figure 7**). Circulating L-EVs were isolated from 3 ml plasma specimens collected at the time of diagnosis from six patients with stage IV EGFR*mut* NSCLC and prior to the start of treatment with erlotinib. For each patient, deeply annotated clinical history, as well as sequencing data/genetic profile of matched tumor tissue, was available to us through Dr. Natale at Cedars-Sinai Medical Center. L-EVs were isolated by differential centrifugation. Total amount of dsDNA in the LO fractions varied significantly among patients (3.6-77.4 ng), with the median dsDNA content of 9.2 ng. Quality control of the L-EV DNA samples was performed using the Agilent 2100 Bioanalyzer High Sensitivity DNA kit (Agilent Technologies) at the Cedars-Sinai's Applied Genomics, Computation and Translational Core and showed the presence of the high molecular weight, high-quality DNA fragments typical of L-EV DNA [4]. After the quality check, targeted DNA sequencing (QIAseq) using the Lung Cancer panel (DHS-005Z, QIAGEN) was performed by QIAGEN Genomics Services, Frederick, MD, USA. For data analysis, we established a collaboration with Dr. Catherine Grasso at Cedars-Sinai Medical Center. Dr. Grasso has contributed to cancer genomics and precision medicine efforts across multiple cancer types. She developed a precision medicine pipeline for using exome data to identify treatment opportunities in the clinic, and also developed a copy number alteration analysis technique for both exome sequencing and targeted sequencing, which was incorporated into routine clinical methodology [5–8].

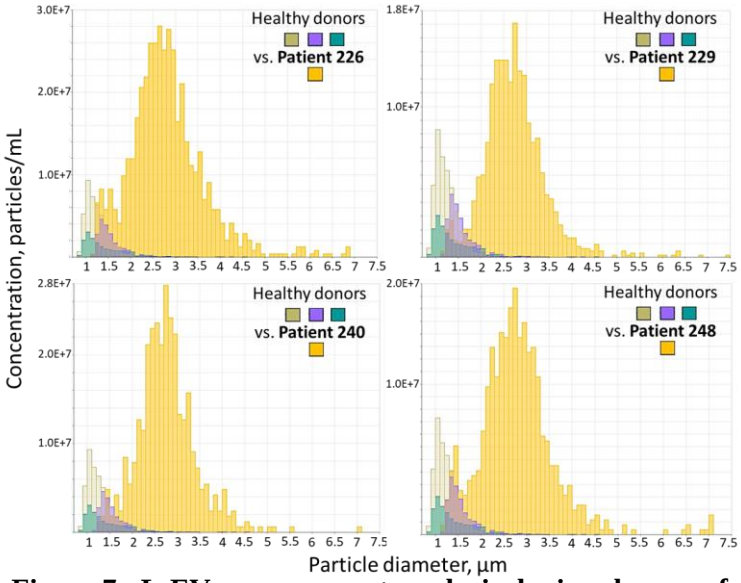

Figure 7. L-EVs are present exclusively in plasma of NSCLC patients. Tunable Resistive Pulse Sensing analysis of plasma samples obtained from four NSCLC patients (yellow) or plasma samples from healthy donors (beige, purple, and turquoise).

Targeted DNA sequencing includes a target enrichment step before the sequencing step. Target enrichment increases the abundance of genes of interest (the lung cancer-associated genes in our case) among the total genomic DNA in the sample. This allows to increase sequencing depth and, thus, to reliably sequence those genes. Many commercially available target enrichment and sequencing methods use PCR amplification processes that introduce artifacts and substantial biases. These artifactual errors significantly limit the detection of true low-frequency variants in heterogeneous DNA samples, such as tumor DNA. To reduce the impact of target enrichment and sequencing artefacts, the QIAseq targeted panels employ molecular barcode technology: each original DNA molecule is attached to a unique molecular index (UMI) prior to PCR amplification for target enrichment. This allows to differentiate between the reads that are sequenced from different original DNA fragments and those arising from PCR artefacts. Thus,

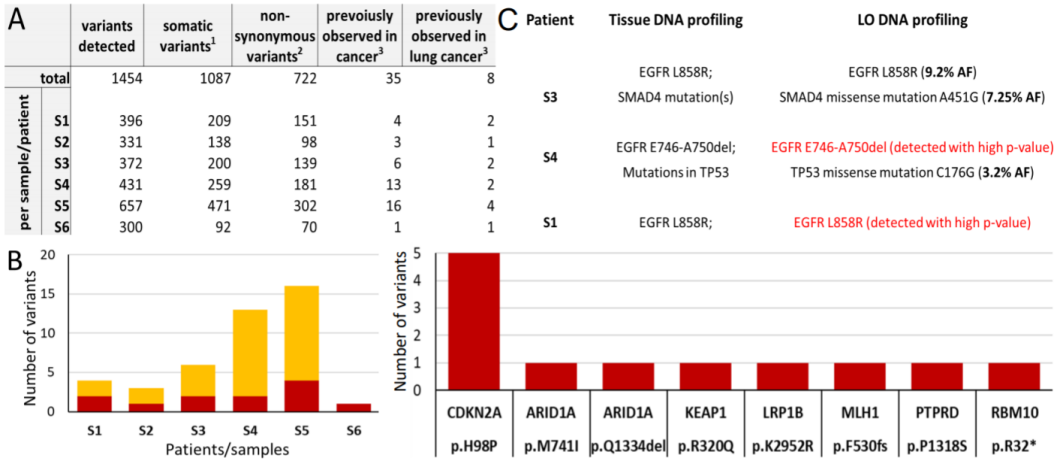

Figure 8. Plasma L-EV DNA obtained from six non-small cell lung cancer (NSCLC) patients reports cancer-specific somatic variants. A. Targeted sequencing using Lung Cancer Panel (DHS-005Z, QIAGEN) of L-EV DNA from 3 ml patient plasma detected a number of somatic variants, including variants previously observed in lung cancer as well as in other cancer types. **B.** Number of detected variants that have been previously observed in lung cancer (red bars) or in other cancer types (yellow bars) for each patient sample. **C.** Previously reported lung cancer variants and their allelic fractions (AF) detection in the study patients.

UMIs allow to detect variants with high sensitivity and accuracy due to a clear discrimination of false positives from true positives [9].

The QIAseq Lung Cancer panel (DHS-005Z, QIAGEN) includes 72 genes and covers all exonic regions plus 10 bases to cover intron/exon junctions. Among all genes covered, we detected a total of 1,454 variants, 1087 (~75%) of which were somatic variants, and 722 (~50%) were non-synonymous variants, meaning that they may have a functional effect (**Figure 8A**). According to Catalogue Of Somatic Mutations In Cancer (COSMIC), the world's largest and most comprehensive resource for somatic mutations in human cancer, out of the non-synonymous variants, 35 (~2.5%) have been previously observed in cancer and 8 (0.55%) have been observed in lung cancer. Among the six patient samples, the number of the cancer- and lung cancer-associated variants ranged between 1-16 and 1-4, respectively, (**Figure 8A, B**). The most frequently detected lung cancer-associated variant, which was found in 5 out of 6 patient samples, was a missense variant in the CDKN2A gene that leads to the substitution of histidine at the position 98 of the CDKN2A protein to proline, p.H98P (**Figure 8B**). Mutations in CDKN2A have been associated with altered sensitivity to the drug Palbociclib *in vitro* [10](Release 8.1 (Oct 2019)). Palbociclib is a Cyclin Dependent Kinase (CDK)4/6 inhibitor that has completed a Phase II clinical trial for treatment of Stage IV NSCLC (https://clinicaltrials.gov/ct2/show/record/NCT01291017). All variants that had been previously observed in lung cancer and their allelic fractios (AF) detected in individual patients are listed in **Table 2**. Finally, a number of genetic alterations detected in circulating L-EVs had also been detected in the tissue biopsies from the same patients (**Figure 4C**), which confirms the feasibility of identification of clinically relevant genomic alterations in circulating LO from EGFR*mut* NSCLC patients.

Table 2. Lung cancer-associated variants and their allele frequencies detected in individual patients

Patient	Gene	Substitution	Annotation	Allele frequency, %
S1	ARID1A	p.M741I	missense variant	3.6
	CDKN2A	p.H98P	missense variant	8.3
S2	CDKN2A	p.H98P	missense variant	5.8
S3	CDKN2A	p.H98P	missense variant	4.4
	MLH1	p.F530fs	frameshift variant	5.8
S4	CDKN2A	p.H98P	missense variant	10.4
	PTPRD	p.P1318S	missense variant	2.8
S5	CDKN2A	p.H98P	missense variant	11.7
	KEAP1	p.R320Q	missense variant	5.3
	LRP1B	p.K2952R	missense variant	5.2
	RBM10	p.R32*	stop gained	4.4
S6	ARID1A	p.Q1334del	disruptive inframe deletion	0.7

References:

1. Reis-Sobreiro, M. *et al.* Emerin Deregulation Links Nuclear Shape Instability to Metastatic Potential. *Cancer Res.* **78**, 6086–6097 (2018).
2. Carreira, S. *et al.* Tumor clone dynamics in lethal prostate cancer. *Sci. Transl. Med.* **6**, (2014).
3. Romanel, A. *et al.* Plasma AR and abiraterone-resistant prostate cancer. *Sci. Transl. Med.* **7**, (2015).
4. Vagner, T. *et al.* Large extracellular vesicles carry most of the tumour DNA circulating in prostate cancer patient plasma. *J. Extracell. Vesicles* **7**, 1505403 (2018).
5. Grasso, C. S. *et al.* The mutational landscape of lethal castration-resistant prostate cancer. *Nature* **487**, 239–243 (2012).
6. Shin, D. S. *et al.* Primary resistance to PD-1 blockade mediated by JAK1/2 mutations. *Cancer Discov.* **7**, 188–201 (2017).
7. Grasso, C. *et al.* Assessing copy number alterations in targeted, amplicon-based next-generation sequencing data. *J. Mol. Diagnostics* **17**, 53–63 (2015).
8. Hovelson, D. H. *et al.* Development and Validation of a Scalable Next-Generation Sequencing System for Assessing Relevant Somatic Variants in Solid Tumors. *Neoplasia* **17**, 385–399 (2015).
9. Peng, Q., Vijaya Satya, R., Lewis, M., Randad, P. & Wang, Y. Reducing amplification artifacts in high multiplex amplicon sequencing by using molecular barcodes. *BMC Genomics* **16**, (2015).
10. Genomics of Drug Sensitivity in Cancer (GDSC): A Resource for Therapeutic Biomarker Discovery in Cancer Cells - PubMed. Available at: https://pubmed.ncbi.nlm.nih.gov/23180760/. (Accessed: 16th June 2020)